

## Current Trends and Emerging Future of Indocyanine Green Usage in Surgery and Oncology: An Update

Jonathan A. Zelken, MD<sup>1,2</sup> and Anthony P. Tufaro, DDS, MD<sup>3,4</sup>

<sup>1</sup>Finesse Plastic Surgery, Orange, CA; <sup>2</sup>Department of Plastic and Reconstructive Surgery, Chang Gung Memorial Hospital, Taoyuan, Taiwan; <sup>3</sup>Department of Plastic and Reconstructive Surgery, The Johns Hopkins Hospital, Baltimore, MD; <sup>4</sup>Department of Oncology, The Sidney Kimmel Comprehensive Cancer Center, The Johns Hopkins Hospital, Baltimore, MD

### ABSTRACT

**Background.** Indocyanine green (ICG) is a widely available dye of clinical importance that has been used for more than 50 years. Near-infrared (NIR) ICG fluorescence imaging has found a niche in cancer care since 2005, and was reviewed in 2011. There is a need for a comprehensive update and we aim to provide this through a review of the most recent literature.

**Methods.** A systematic review of the literature using PubMed, EMBASE, and MEDLINE databases of articles published from 2000 to June 2015 evaluated topics pertinent to NIR fluorescence imaging with ICG in the diagnosis and surgical treatment of cancer. Articles previously referenced in a 2011 review and a 2015 meta-analysis were excluded, while articles that referenced future directions and economics were included in this current review.

**Results.** Since 2011, the literature has grown exponentially, with significant advances at the molecular level. Significant findings from 89 select articles and 10 reviews, most of which were published between 2011 and 2015, are summarized. Preclinical studies are currently underway investigating tumor-specific fluorescence and targeted therapeutic delivery. The potential for ICG exists at every level of cancer care, from diagnosis to surveillance.

**Conclusion.** The indications, applications, and potential for ICG have grown exponentially in the past decade; an updated review of the literature is overdue and we present the most comprehensive review to date.

In the war against cancer, myriad emerging technologies offer promise in improving accuracy and efficiency in cancer diagnosis, treatment, reconstruction, and surveillance. One medium has existed for the better part of a century and has proven feasible in accomplishing every aforementioned goal. Indocyanine green (ICG) was introduced as a photographic dye after World War II, before hepatologists, cardiologists, nephrologists, and ophthalmologists used it as a diagnostic aid. Decades later, the dye was rediscovered as a fluorophore that absorbed and emitted light in the near-infrared (NIR) spectrum. Co-evolution of imaging technologies has generated a powerful tool that has found its place in almost every surgical field and at every level of comprehensive cancer care, from diagnosis to reconstruction.

After a quick PubMed search query for ‘ICG’, it is plain to see that the number of topical articles has grown exponentially, with paradigm shifts in its utility as a dye, a fluorophore, and a perfusion assessment aid (Fig. 1). Today a ‘fourth paradigm’ of ICG use is its role in so-called *theranostic* nanoparticles that diagnose and treat cancer. Preclinical trials of ICG-loaded nanoparticles for tumor-specific diagnosis and therapy are underway.<sup>1–13</sup> In 2011, Polom et al. presented a thoughtful review of the trends and future directions of ICG in surgical oncology, focusing on its role as an NIR fluorophore that facilitates sentinel lymph node (SLN) mapping.<sup>14</sup> Since then, many series have been published.

In a recent meta-analysis, Xiong et al. reported 96 % SLN detection using NIR fluorescence, with 86 % sensitivity and 100 % specificity of various tumors citing 15 series.<sup>15</sup> However, to the authors’ knowledge, ICG fluorescence imaging and its role in the war against cancer has not been comprehensively summarized since 2011.<sup>14</sup> An organized update is overdue. To accomplish this, a

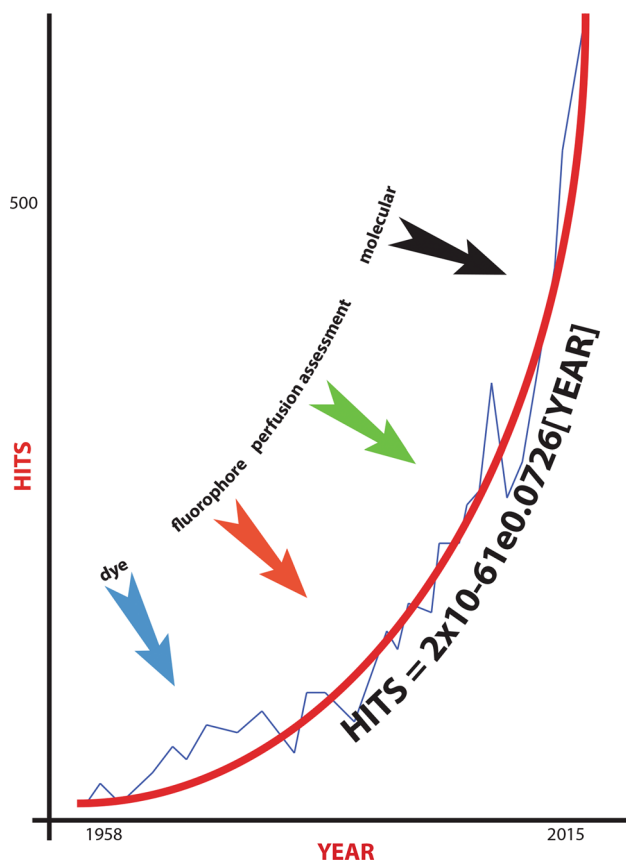


**FIG. 1** The number of PubMed-listed publications ('HITS') for the term 'indocyanine green' approximates the curve:  $HITS = 2 \times 10^{-61}e^{0.0726[YEAR]}$  ( $R^2 = 0.83$ ). ICG was a diagnostic dye (blue arrow), then a fluorophore (red arrow). At the turn of the millennium, ICG was rediscovered for perfusion assessment (green arrow), and modern research is investigating its role in cancer imaging and treatment ('the fourth paradigm', black arrow). ICG indocyanine green (Color figure online)

systematic review of the literature was designed and executed to summarize the most current recommendations, applications, and innovations for ICG fluorescence imaging in the context of cancer care. The economics of ICG imaging, as well as future directions and technologies, are discussed in this update.

## METHODS

A literature search was performed in June 2015 using the MEDLINE, EMBASE, and PubMed databases. The PubMed search was performed using Medical Subject Headings (MeSH) and keywords, while the EMBASE and Medline searches were performed using MeSH terms and free terms. Search queries and results are summarized in Table 1. Terms were chosen to capture every potentially

relevant article that might resemble or relate to the use of ICG fluorescence imaging in the diagnosis and treatment of cancer, from nanoparticles to free flaps. The search was restricted to post-millennial studies (1 January 2000–2 June 2015) to limit articles to relevant technologies and methods. Articles not available in English were excluded. Articles without abstracts, case reports, and non-human studies were excluded. Articles that contained redundant data from previously reported series were excluded if the conclusions did not change. PRISMA (Preferred Reporting Items for Systematic Reviews and Meta-Analyses) guidelines were respected in the execution and delivery of this update and review.<sup>16</sup>

## Inclusion Criteria

For each search result, the title, abstract, and authorship panel were screened for potential relevance using the following inclusion criteria: the article reported on novel or established applications of ICG imaging in the diagnosis and surgical treatment of cancer. Additional topics of interest were anatomical imaging methods, economics of ICG imaging, clinical outcomes, and comparisons with currently accepted methods. Because this review was intended to provide an update, not a reiteration, of previous work, series of ten or more patients where ICG was used for SLN mapping were included if they were not already discussed in the reviews by Xiong et al.<sup>15</sup> and Polom et al.<sup>14,17,18</sup> To ensure all relevant articles were included a second 'pass' was performed by scanning reference lists of the included articles.

Figure 2 illustrates the selection process for articles included in this review. Potentially relevant articles were identified from a pool of 1626 results on the basis of title and abstract. The quality of the articles were assessed qualitatively and on the basis of the number of patients studied, follow-up time, study purpose and design, identifiable biases, command of the English language, and thoroughness. In several instances, the objectives and topic of papers were unclear. For these articles, and those that passed the first screening, full-text versions were obtained. A total of 1524 articles were screened out for failure to meet the inclusion criteria. The second pass added three articles with content that was relevant to this update.<sup>19–21</sup>

## Data Interpretation

Articles were broadly categorized as diagnostic/therapeutic (breast, hepatobiliary, skin, enteric, genitourinary, lung, other), economic, reconstructive, and technologic.

**TABLE 1** Literature search

Search type	Query or terms used	Hits <sup>a</sup> PubMed	Hits <sup>b</sup> EMBASE
MeSH terms	(((indocyanine green) OR ICG) OR fluorescent dyes) OR dyes)) AND (((((((((((((((laparoscopy) OR laparoscopic) OR laparoscopic surgery) OR robotic) OR robot-assisted) OR robotic surgery) OR robot-assisted surgery) OR minimally invasive) OR endoscop*) OR endoscopic surgery) OR minimally invasive surgery) OR cancer surgery) OR surgical oncology) OR extirpation) OR excision) OR resection) OR *ectomy) OR robot-assisted surgery)) AND (((((((breast cancer) OR skin cancer) OR cancer) OR tumor) OR neoplas*) OR metasta*) OR recurrence)) AND (((near-infrared) OR NIR) OR near-infrared fluorescence imaging) OR fluorescence imaging)) AND ((Fluorescent Dyes [MeSH Terms]) OR indocyanine green [MeSH Terms]))	398 <sup>c</sup>	–
Keyword terms	'surgery'/exp OR 'cancer surgery'/exp OR 'sentinel lymph node biopsy'/exp AND 'neoplasm'/exp AND ('indocyanine green'/exp OR 'icg'/de) AND ([article]/lim OR [review]/lim) AND [humans]/lim AND [english]/lim AND [abstracts]/lim AND [2000-2015]/py	–	593
Free terms	Near-infrared AND oncology	109	81
	Near-infrared AND lymph node AND mapping	58	53
	Near-infrared AND sentinel lymph node	86	130
	Indocyanine green AND oncology	113	88
	Indocyanine green AND lymph node AND mapping	76	70
	Indocyanine green AND sentinel lymph node	172	219
	Fluorescence AND lymph node AND mapping	124	60
	Fluorescence AND sentinel lymph node	190	129
	<i>Total (without duplicates)</i>	<i>n = 749</i>	<i>n = 877</i>

MeSH Medical Subject Heading

<sup>a</sup> Last search conducted on 2 June 2015

<sup>b</sup> Last search conducted on 2 June 2015

<sup>c</sup> Filtered (date: 2000–; language: English; contains abstract; species: humans)

Breast cancer was further categorized as SLN, lymphedema, and margin control. Enteric cancer-related articles were further categorized as extirpative and reconstructive. The major focus or message of the studies was described and a summary statement was synthesized for each topic. No meta-analysis was attempted given the significant heterogeneity of studies, organ systems, and outcomes measures.

**RESULTS**

Since 2000, a total of 99 papers, including 89 study reports and 10 review articles, were published that met the criteria for this review. Although inclusion criteria and methodology for the review were not stated, only two articles of potential relevance were identified but were not included in the exhaustive 2011 review by Polom et al.<sup>22,23</sup> A total of 26 series relevant to SLN mapping were identified that were not included in prior reviews and meta-analyses by Polom et al. and Xiong et al. (Table 2).<sup>14,15,24</sup> Broadly, the geographic focus of studies seems to have shifted westward, with a waning role in gastrointestinal staging and an expanding role in minimally invasive surgery, urology, and gynecology. A synthesis of each topic was agreed upon by the authors and is listed in Table 3.

**BREAST CANCER**

*Sentinel Lymph Node Mapping*

ICG is used in SLN mapping in the same manner as radioisotope (RI) and dye; it is instilled subdermally and drainage patterns are tracked. Ahmed et al. reviewed 15 articles comparing NIR fluorescence imaging with conventional methods of SLN mapping in breast cancer.<sup>25</sup> Acknowledging heterogeneity in study design and short follow-up, the authors reported that ICG was better than blue dye for SLN identification, ICG and RI were comparable for node identification, and further study comparing ICG with the conventional dual RI-dye method was warranted. In 2014, Inoue et al. reported a 99.6 % SLN detection rate and a 0.4 % false-negative rate with ICG and blue dye in a well-designed study of 714 patients.<sup>26</sup> The authors felt ICG dye could replace RI dye, and ICG has been endorsed in other studies.<sup>27–32</sup> Most recently, Samorani and co-workers presented a series of 301 women in whom ICG methods were compared with RI. Of the 589 nodes removed in that series, 99 % were identified with ICG, while 77 % were identified with RI. There was a 99 % concordance between RI and ICG. Seventy metastatic nodes were biopsy-proven: 21 % of nodes were fluorescent

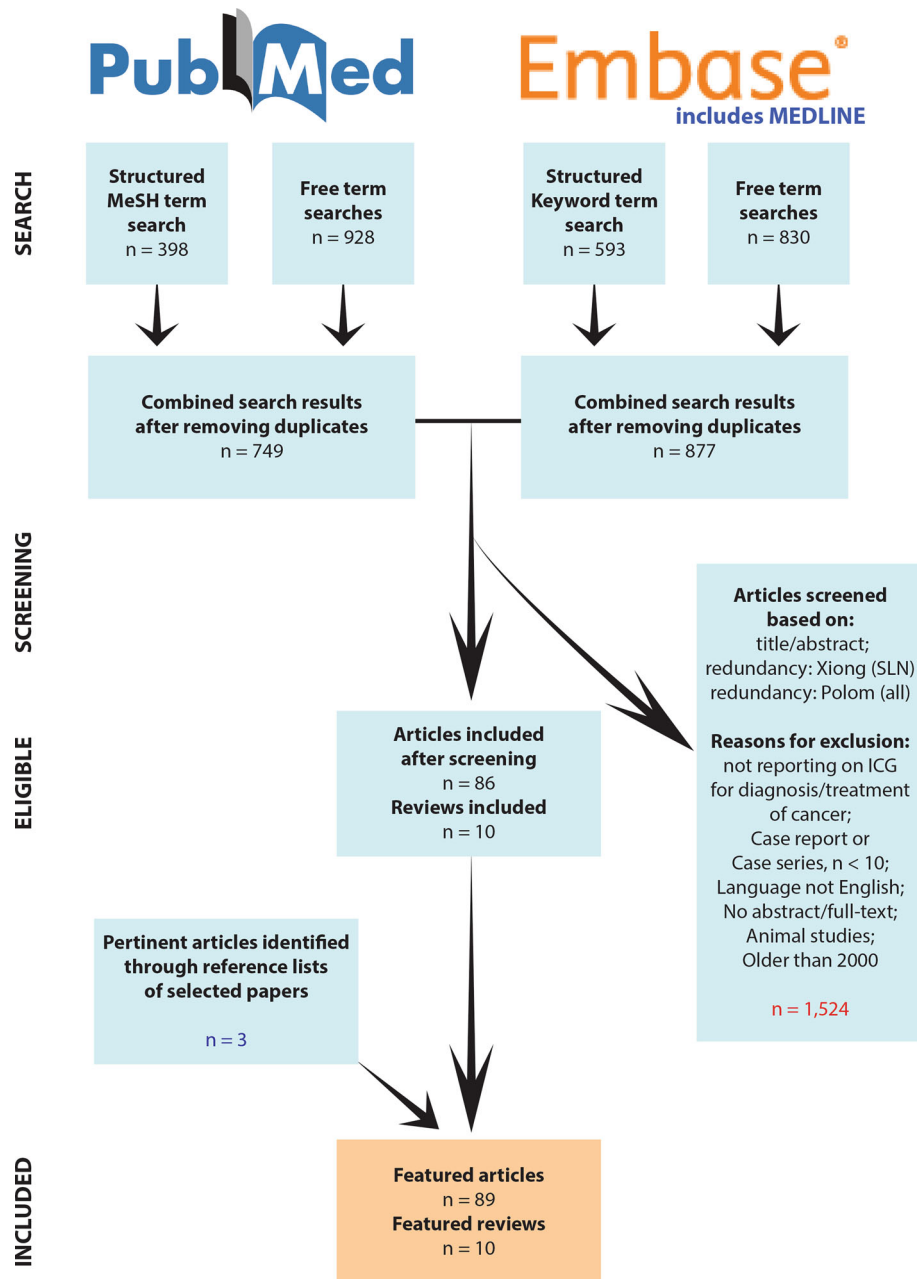


**FIG. 2** Systematic literature search and inclusion methodology. *MeSH* Medical Subject Heading, *ICG* indocyanine green, *SLN* sentinel lymph node

but cold (thus, ICG benefited six patients). None were hot, and were not fluorescent (0 % ICG false-negatives).<sup>33</sup>

### Lymphedema

Axillary reverse mapping (ARM) is accomplished by subdermal instillation of dye in the breast and ipsilateral arm, and comparison of drainage patterns. ARM can prevent lymphedema after lymph node dissection (LND) when separate arm and breast drainage patterns exist.<sup>34,35</sup> Guided by NIR fluorescence imaging, Sakurai et al.<sup>36</sup> followed

women whose arm lymphatics were both spared and not spared. The majority (76.8 %) of 321 women had separate drainage patterns. Arm lymphatics were not spared in 76 women with overlapping drainage, and five developed lymphedema. In the remaining 245 women, none developed lymphedema ( $p < 0.0001$ ). ICG increased the sensitivity of ARM compared with dye alone, and the time and ICG cost was minimal. Ikeda et al. evaluated the significance of positive ARM nodes in axillary LND. In a series of 101 patients, ARM nodes were identified in 76 patients. Metastatic ARM nodes were confirmed in 42 and

**TABLE 2** Relevant series (2000–2015) not included in previous reviews with >10 patients using ICG for SLN mapping

Author	Objective	N	ICG dose/conc	SLN detection, patients (%)	False-negatives (%)	Remarks
Cloyd et al. <sup>66</sup>	Melanoma	52	2 ml 0.25 % ICG	46/52 (88.5)	2/11 (18.2)	ICG increases sensitivity
Inoue et al. <sup>26</sup>	Breast	714	1 ml 0.5 % ICG	711/714 (99.6)	–	ICG + BD > ICG + RI
Tong et al. <sup>29</sup>	Breast	96	2 ml 0.5 % ICG	93/96 (96.9)	1/29 (3.4)	ICG + BD > ICG
Schaafsma et al. <sup>82</sup>	Bladder	12	2 ml ICG:HSA	11/12 (92)	0	ICG:HSA proof of concept
Manny et al. <sup>83</sup>	Prostate	50	0.8 ml 2.5 % ICG	38/50 (76)	0	ICG is highly sensitive, nonspecific
Korn et al. <sup>59</sup>	Melanoma	50	0.5–1.5 ml 0.25 % ICG	49/50 (96)	0	Higher sens/spec than other methods
Jewell et al. <sup>77</sup>	Uterine	227	4 ml 0.125 % ICG	216/227 (95)	–	ICG > BD
Verbeek et al. <sup>30</sup>	Breast	95	1.6 ml 0.5 % ICG	94/95 (99)	0	ICG or RI: gold standard?
Guo et al. <sup>27</sup>	Breast	36	1 ml 0.5 % ICG	35/36 (97.2)	1/19 (5.3)	ICG > BD
Miyashiro et al. <sup>69</sup>	T1 gastric	440	4–5 ml 0.5 % ICG	304/311 (97.7)	13/28 (46)	Unacceptable FNs (suspended trial)
Sugie et al. <sup>31</sup>	Breast	99	0.5–1 ml 0.25 % ICG	98/99 (99.6)	0	ICG > BD
Ballardini et al. <sup>32</sup>	Breast	134	1 ml 0.5 % ICG	245/246 nodes (99.6)	–	ICG validated against RI
Gilmore et al. <sup>88</sup>	NSCLC	37	3.8–2500 µg ICG	15/37 overall (40) 8/9 if >1 g ICG (89)	0	ICG dose > 1000 µg recommended
van der Pas et al. <sup>68</sup>	Colon	14	1 ml ICG:HSA	14/14 (100)	4/14 (28.6)	ICG is safe + feasible
Gilmore et al. <sup>58</sup>	Melanoma	25	1 ml 0.1–0.5 % ICG:HSA	24/25 (96)	–	ICG:HSA feasible and accurate
Schaafsma et al. <sup>81</sup>	Vulvar	24	1.6 ml ICG or ICG:HSA	35/35 nodes (100)	–	ICG:HSA = ICG
van der Vorst et al. <sup>60</sup>	Melanoma	15	1.5 ml ICG varied dose	14/15 (93)	–	600 µM = best ICG dose
Hirano et al. <sup>28</sup>	Breast	501	2.5 ml 0.2 % ICG	501/501 (100)	0	ICG is useful when RI is not available
Jain et al. <sup>61</sup>	Melanoma	15	1–2 ml 0.25 % ICG	13/15 (87)	0	ICG is a reasonable alternative to RI
Miyashiro et al. <sup>69</sup>	T1/T2 gastric	241	4–5 ml 0.5 % ICG	240/241 (99.6)	3/29 (10.3)	ICG a good adjunct in T1/T2 cancer
Fujisawa et al. <sup>65</sup>	Skin cancer	34	0.4–0.8 ml 0.5 % ICG	33/34 (97)	0	ICG reduces false-negatives
Stoffels et al. <sup>63</sup>	Skin cancer	22	1 ml 0.2 % ICG	22/22 (100)	0	ICG reduces false-negatives
Namikawa and Yamazaki <sup>64</sup>	Melanoma	49	1 ml 0.5 % ICG	49/49 (100)	0	ICG reduces false-negatives
Yamashita et al. <sup>84</sup>	NSCLC	61	2 ml 0.5 % ICG	49/61 (80.3)	1/49 (2.1)	RT-PCR may enhance diagnosis
Crane et al. <sup>78</sup>	Vulvar	10	1 ml 0.5 % ICG	10/10 (100)	0 %	ICG > BD
Samorani et al. <sup>33</sup>	Breast	301	0.3–1.4 ml 0.5 % ICG	583/589 nodes (99)	0 %	ICG could be validated as an alternative to RI

NSCLC non-small cell lung cancer, ICG indocyanine green, HSA albumin, BD blue dye, RI radioisotope, FNs false-negatives, sens/spec sensitivity and specificity, RT-PCR real-time polymerase chain reaction, SLN sentinel lymph node, conc concentration, – indicates not measured

13 % of patients who developed lymphedema and those who did not, respectively. The odds ratio was 3.61, but those who developed lymphedema were treated more frequently with postoperative radiation.<sup>37</sup> After endorsing the feasibility of ARM,<sup>38,39</sup> Noguchi et al. reviewed the literature and spoke on the oncologic safety of ARM when the SLN is not clinically positive and the upper extremity and breast drainage pathways are isolated.<sup>40</sup>

Should lymphedema develop, treatment strategies include lymphatic bypass procedures and microsurgical transfer of

vascularized lymph node basins that reduce limb circumference and improve quality of life.<sup>41–46</sup> An emerging controversy is donor site morbidity and, more specifically, iatrogenic lymphedema.<sup>47,48</sup> Dayan and colleagues use technetium and ICG to reduce the incidence of iatrogenic lymphedema caused by transferring functionally predominant lymph nodes in vascularized lymph node transfer. With his method, a donor groin lymph node flap is identified by ICG fluorescence, and abandoned if it contains a gamma-positive SLN, or ‘hot spot’ from the ipsilateral lower extremity.<sup>49</sup>

**TABLE 3** Summary of studies referenced

Topic	Summary
Breast cancer	ICG imaging has a role in breast cancer identification, sentinel lymph node biopsy with low false-negative rate, margin control, reconstruction, lymphedema prophylaxis and treatment
Liver cancer	ICG is a good adjunct to standard diagnostics for liver cancer treatment, is best for small, superficial, and metastatic lesions, has the potential to aid the pathologist, and may suggest the degree of tumor differentiation
Skin cancers	NIR fluorescence-guided LND is possible in the vast majority of skin cancer patients, and false-negatives approach nil
Enteric cancers	ICG fluorescence imaging can aid SLN detection, high false-negatives should be anticipated, and NIR fluorescence is more reliable in low-stage gastric, colorectal, and anal cancer. Following extirpation and mapping, the same technology is a useful perfusion assessment aid, but the influence of the technology on outcomes has yet to be determined
Genitourinary cancers	Clinical studies are promising but inconclusive in prostate cancer, NIR fluorescence imaging enhances sensitivity in SLN mapping, NIR fluorescence imaging may be superior to blue dye in cervical and uterine SLN mapping, NIR fluorescence imaging is compatible with robotic surgery and current technologies support its use
Lung cancer	NIR fluorescence imaging is safe and effective for NSCLC staging but further study is warranted to identify a meaningful role. There may be a role for fluorescence imaging as an adjunct to visual inspection and palpation in the surgical management of pulmonary nodules and metastatic lung cancer
Cancer reconstruction	There is a role for NIR fluorescence imaging in cancer reconstruction with the potential to reduce costs, improve outcomes, and eliminate unnecessary surgery
Future directions	ICG-loaded nanoparticles are exciting potential 'theranostic' agents, and are currently in preclinical trials

ICG indocyanine green, NIR near-infrared, LND lymph node dissection, SLN sentinel lymph node, NSCLC non-small cell lung cancer

### Margin Control

Tummers et al. used NIR fluorescence imaging with methylene blue (MB) for lumpectomy to identify wound margins after intravenous instillation of dye. They described a case where neither specimen nor wound bed fluoresced; the specimen was divided and its fluorescent core suggested clear margins. In another case, patchy specimen and wound bed fluorescence suggested inadequate resection.<sup>50</sup> Like ICG, MB fluoresces in the NIR range. Its tumor-seeking mechanism is unclear but, like <sup>99m</sup>Tc-MIBI,<sup>20</sup> MB is lipophilic and passively enters apoptotic and proliferating cells with large negative membrane potentials.<sup>51</sup> In an animal model, Madajewski et al. used ICG fluorescence to image wound beds after tumor resection, and identified residual tumor not otherwise visible to the naked eye<sup>52</sup>; a phase I/II clinical trial for patients undergoing breast and lung cancer resection is ongoing.

### LIVER CANCER

ICG is hepatically cleared and masses influence biliary flow; flow distortions after intravenous dye administration may guide hepatic resection.<sup>53</sup> In 2009, Ishizawa et al. identified 8 of 63 hepatocellular carcinomas (HCCs) with NIR fluorescence imaging that were otherwise imperceptible; few false-positives were identified (8 %).<sup>22</sup> By 2014, the series grew to 170 subjects and 276 HCCs. NIR fluorescence identified 273 of 276 lesions (99 %), including 21 grossly unidentifiable lesions. Three false-negatives (1 %) were identified.<sup>54</sup> van der Vorst et al. identified lesions in 5 of 40 patients with NIR imaging that were missed by

intraoperative ultrasound, palpation, inspection, and preoperative computed tomography (CT).<sup>55</sup>

Kawaguchi et al. described identifiable fluorescence patterns that resulted from differentiation-dependent hepatocyte dysfunction.<sup>21</sup> Well-differentiated tumors were capable of absorbing ICG but multidrug resistance-associated protein 2 (MRP2) transporter dysfunction prohibited excretion, resulting in homogenous fluorescence.<sup>19</sup> Poorly differentiated and metastatic tumors did not absorb (faulty OATP/NTCP channel) or excrete dye, generating a 'halo sign' of rim fluorescence.<sup>55</sup> Lim et al. used NIR fluorescence to distinguish benign and malignant lesions and identify small superficial lesions.<sup>56</sup> Tummers et al. used laparoscopic NIR technology to image hepatic uveal melanoma metastases; two of three lesions were not visualized on preoperative imaging.<sup>57</sup>

### SKIN CANCER

NIR fluorescence-guided LND is possible in the vast majority of skin cancer patients, and false-negatives approached nil. Since 2011, at least seven series of NIR fluorescence imaging of skin cancer have emerged.<sup>58–65</sup> However, no conclusive or long-term evidence that NIR fluorescence imaging is superior to current techniques exists. Because NIR fluorescence imaging is highly sensitive it may be superior for detecting small nodes overlooked by RI and dye.<sup>63,64,66</sup> Additionally, NIR fluorescence imaging tracks lymphatic flow in real-time and may reduce false-negatives in conjunction with current methods. NIR fluorescence fails when lymphatics cannot be visualized.<sup>67</sup>

## ESOPHAGEAL, GASTRIC, COLORECTAL, AND ANAL CANCER

### *Extirpation*

According to Xiong and colleagues,<sup>15</sup> sensitivity and SLN detection with NIR fluorescence imaging was comparable with RI dye for gastric cancer. Low sensitivity and high false-negatives with both were attributed to the complex architecture of gastric lymphatics and the skip metastasis phenomenon. Three studies detailing NIR fluorescence imaging for treatment of gastric cancer have since been published.<sup>24,68,69</sup> Miyashiro et al. presented 241 patients with T1 and T2 gastric cancer<sup>69</sup> and detected SLNs in 99.7 % of patients, with a 10.3 % false-negative rate. A subsequent clinical trial in patients with T1 cancer was set at 1550 patients across multiple centers in Japan to validate NIR fluorescence imaging against histological data; however, accrual was suspended early because of an unacceptably high false-negative rate (46 %), which the authors attributed to an inadequate learning period and poor frozen section analysis. They supported NIR fluorescence-based SLN mapping but contended that better methods of frozen specimen analysis were needed to prove it. Noura et al. detected a 92 % rate of SLNs in anal cancer irrespective of tumor stage,<sup>70</sup> with no false-negatives; NIR fluorescence imaging was better than RI and dye.<sup>71</sup> Kusano reported a 67 % false-negative rate with NIR fluorescence-based SLN mapping in T2 colon cancer. van der Pas et al. used NIR fluorescence imaging to identify SLNs in 14 of 14 patients with colon cancer; however, there were four false-negatives (29 %).<sup>68</sup> Despite this false-negative rate, the authors supported laparoscopic SLN mapping in colon cancer and attributed false-negatives to the learning curve and procedural difficulties.

**Reconstruction** ICG fluorescence imaging can be used for perfusion assessment in esophageal and gastrointestinal reconstruction.<sup>72–74</sup> Shimada et al. assessed perfusion of reconstructed organs with the technology, and determined whether vascular supercharging was needed.<sup>75</sup> The technology was feasible in every case but the anastomotic leak rate was not significantly improved with implementation. Ultimately, perfusion assessment was accomplished but the clinical relevance of perfusion (the adequacy of that perfusion to predict tissue viability) was not determined.

## GENITOURINARY CANCERS

Xiong et al. summarized four well-designed series that investigated NIR fluorescence imaging for the treatment of genitourinary cancers<sup>15</sup>; the authors were underwhelmed by the low sensitivity of NIR fluorescence imaging in that

context. Over one dozen series on NIR fluorescence-based SLN mapping of prostate, bladder, vulvar, uterine, and cervical cancers have since been published.

In 2014, Handgraaf et al.<sup>76</sup> reviewed five vulvar cancer series ( $n = 70$  patients) and seven endometrial cancer series ( $n = 121$  patients). NIR fluorescence imaging enhanced sensitivity in vulvar cancer SLN detection but radiotracers were indispensable for localization. NIR fluorescence imaging was feasible in endometrial cancer treatment and could replace blue dye. Jewell et al. corroborated these data in a study of 227 women with uterine and cervical cancer; SLNs were detected in 95 % of patients and blue dye was unnecessary when ICG was used.<sup>77</sup> Crane et al. favored ICG over dye in a study of ten lean women with vulvar cancer,<sup>78</sup> while Sinno et al. advocated NIR fluorescence-based SLN detection over dye in women with endometrial cancer and increased BMI.<sup>79</sup> Schaafsma et al. compared ICG conjugated with albumin (ICG:HSA) with ICG in 24 vulvar cancer patients; HSA was expected to enhance detection because of increased lymphatic uptake.<sup>80–82</sup> All 35 nodes were identified in both groups and ICG:HSA did not appear to confer an advantage over ICG alone.

Manny et al. detected SLNs in 38 of 50 men (76 %) with prostate cancer using robot-integrated NIR fluorescence imaging<sup>83</sup>; SLN detection was nonspecific (75 %) but sensitive (100 %) for nodal metastasis. The authors did not consider NIR fluorescence imaging superior to current methods, and were enthusiastic about time and cost savings when ICG was used as an intraoperative tumor marker compared with ultrasound and cystoscopy.

## LUNG

Yamashita et al. used thoracoscopic NIR fluorescence imaging for non-small cell lung cancer (NSCLC) and detected 80.6 % of SLNs, with no false-negatives,<sup>84</sup> compared with 50 and 64 % SLN detection for RI and blue dye, respectively.<sup>85</sup> NIR fluorescence imaging was faster, less expensive, and had a reduced tendency to miss regional metastasis than CT or positron emission tomography (PET).<sup>86</sup> Yamashita et al. enhanced their protocol with intraoperative real-time polymerase chain reaction for CK-19 expression,<sup>87</sup> but SLN detection and false-negative rates were comparable with previous data. In a phase I ICG dose-escalation trial for open and thoracoscopic NIR fluorescence-based SLN mapping of NSCLC, Gilmore et al. detected 90 % of SLNs when 1000  $\mu\text{g}$  ICG or greater was given, and no false-negatives were observed.<sup>88</sup> Okusanya identified pulmonary nodules *intraoperatively* using ICG fluorescence imaging in a series of 18 patients. Overall, 16 of 18 nodules identified by visual inspection and manual palpation were detected with fluorescence imaging, but

fluorescence imaging also identified five subcentimeter nodules and five metastases that were not found by inspection and palpation.<sup>89</sup>

## OTHER APPLICATIONS

Yokoyama et al. explored the feasibility of NIR fluorescence-guided head and neck cancer surgery.<sup>90</sup> The authors demonstrated tumor fluorescence lasting 6 h, and suggested lesion-specific uptake was a result of peritumoral vascular hyperpermeability. Overall, 30–60 min were required to appreciate a contrast between normal and diseased tissue after ICG injection, and visualization was best from 60 to 120 min. Ohba et al. used NIR fluorescence imaging to administer superselective intra-arterial chemotherapy. Compared with CT, NIR fluorescence imaging provided clearer, more precise images without dental metal-related scatter. A feeding vessel was identified in 100 % of 25 cases versus 56 % with CT.<sup>91</sup> In a similar study, Yokohama et al. visualized a feeding vessel in 47 % of 36 cases of paranasal sinus cancer with CT versus 100 % with NIR fluorescence imaging.<sup>92</sup>

Watanabe et al. recommended ICG for preoperative colonic tattooing. It was cleaner than blue dye, had fewer side effects and histologic artifact, lasted up to 14 days, and was detected in 100 % of cases.<sup>23</sup> Hao et al. used microscope-integrated NIR technology to facilitate resection of a dorsal spinal hemangioma,<sup>93</sup> while Holt et al. observed distinct fluorescence patterns in healthy and diseased tissue in lung cancer, sarcoma, carcinoid, and thymoma. These observations were duplicated in an animal study but the authors warned inflammation and tumor fluorescence might be indistinguishable.<sup>94</sup>

## ADDITIONAL BENEFITS

Furukawa used NIR-guided imaging to assess skin perfusion in 17 patients undergoing inguinal LND and excised skin that did not fluoresce.<sup>95</sup> More than 1 cm wound dehiscence persisted for 3 weeks in seven of nine patients who did not receive ICG-guided intervention. In contrast, one of eight patients with ICG-guided skin trimming dehisced ( $p < 0.003$ ). Other examples of NIR-guided reconstruction are described for breast and esophageal cancer.<sup>72–75</sup>

## ECONOMIC CONSIDERATIONS

NIR guidance has the potential of reducing healthcare expenditure if improved outcomes warrant replacement of current technologies at a reduced unit cost. Lymphoscintigraphy is the standard for detecting nodal metastasis, but it is invasive, false-negatives exceed 5 %, radiation is detected,

and it is costly and time consuming.<sup>96</sup> Many commercially available charge-coupled device (CCD) cameras exist, with different pricing structures. The price of the Photodynamic Eye device (PDE; Hamamatsu Photonics Co., Hamamatsu City, Japan) has been cited elsewhere.<sup>97,98</sup> Alternatively, the Spy Elite system (Novadaq Technologies, Mississauga, ON, CAN) is reported per use; depending on the financial arrangement, supply kits—not the unit itself—generate cost.<sup>99–101</sup> ICG is inexpensive, therefore marginal cost can be quite low.<sup>97,102</sup> Because wide variations exist in pricing and cost structure (Table 4), cost-utility analyses may be unreliable. In relevant studies, it was difficult to understand how cost was defined.<sup>103–110</sup> Additional considerations include medicolegal ramifications, depreciation, and the monetary value of time spent scheduling, staffing, and in the operating room.

Duggal et al. demonstrated that indiscriminate use of NIR-guided imaging in breast reconstruction saved patients US\$610 by decreasing the rate and extent of skin flap necrosis and reducing unplanned hospitalizations.<sup>100</sup> Kanuri et al. recognized potential cost savings when ICG was reserved for high-risk patients (smokers, obese subjects, and large-breasted subjects) and not used indiscriminately.<sup>101</sup> Yeoh et al. predicted additional economic benefits with widespread use, citing reduced technology costs and fewer complications.<sup>111</sup>

## RECONSTRUCTION

Data support NIR-guided breast reconstruction. In the series by Komorowska-Timek and Gurtner, NIR fluorescence imaging reduced the flap necrosis rate from 15.4 to 4 % when used during all stages of breast reconstruction.<sup>112</sup> Newman and co-workers demonstrated a 95 % correlation between intraoperative imaging and outcome after 20 mastectomies.<sup>113</sup> Moyer and Losken used analytic software (Spy-Q; Novadaq Technologies) to quantify flap fluorescence relative to surrounding tissue; tissue with  $\geq 45$  % relative fluorescence had a higher chance of surviving.<sup>114</sup> Other authors have used 30 % as a cutoff.<sup>115</sup>

Holm et al. used NIR-guided imaging to examine microvascular anastomoses in a series of patients taken back to the operating room for concern regarding flap failure. Anastomoses were revised regardless of ICG results, and imaging data was validated against intraoperative findings. NIR imaging was 100 % sensitive and 86 % specific for microvascular thrombosis.<sup>116</sup> Khansa et al. incorporated NIR fluorescence imaging into their failing free-flap algorithm.<sup>117</sup> When there was venous congestion but NIR imaging revealed a patent venous anastomosis, thrombolysis was administered. With arterial compromise, ICG was used to identify the obstruction to inflow.



**TABLE 4** Economics of indocyanine green

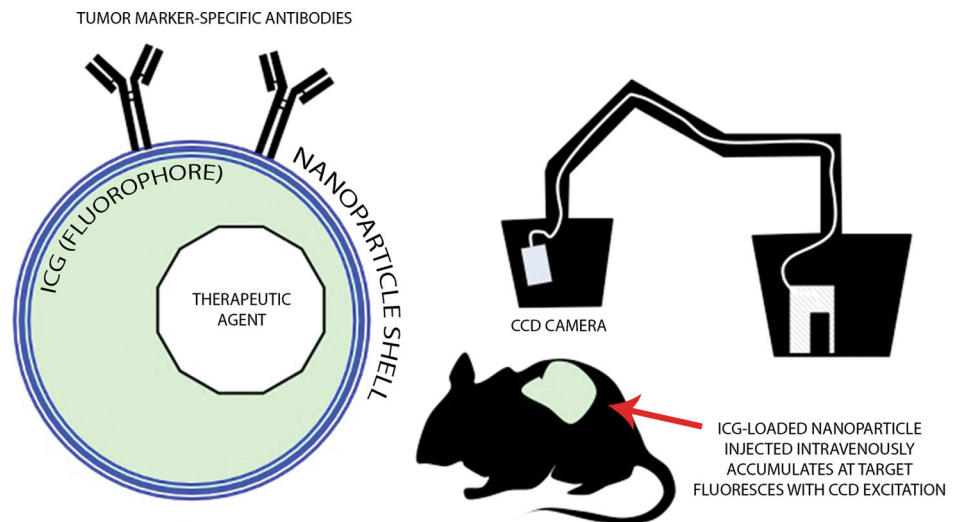
Author	Year	Indication	Nation	Cited cost	Currency year	Corrected to 2014 US\$ <sup>a</sup>	Pricing
<b>Nuclear imaging</b>							
McMasters et al. <sup>107</sup>	2000	Breast cancer	USA	US\$706	2000	943.56	Per case
Jakovljevic et al. <sup>104</sup>	2013	Cancer	Serbia	€940	2013	1145.51	Per case
Govers et al. <sup>103</sup>	2013	Oral cancer	Netherlands	€210	2011	315.28	Per case
Martinez-Menchon et al. <sup>105</sup>	2014	Melanoma	Spain	€200.38	2014	244.19	Per case
Meads et al. <sup>108</sup>	2013	Vulvar cancer	UK	£645 <sup>b</sup>	2010	1071.83	Per case
O'Connor et al. <sup>109</sup>	2013	Oral cancer	UK	€378	2013	521.69	Per case
Thompson et al. <sup>110</sup>	2008	Breast cancer	USA	US\$1434	2008	1547.42	Per case
McCann et al. <sup>106</sup>	2014	Vulvar cancer	USA	US\$408.96 <sup>c</sup>	2013	408.96	Per case
<b>NIR fluorescence</b>							
<b>SPY (Novadaq)</b>							
Duggal et al. <sup>100</sup>	2014	Breast reconstruction	USA	US\$795	2014	795	Per case
Kanuri et al. <sup>101</sup>	2014	Breast reconstruction	USA	US\$650	2011	693.14	Per case
Chatterjee et al. <sup>99</sup>	2011	Breast reconstruction	USA	US\$1195	2011	1274.31	Per case
<b>PDE (Hamamatsu)</b>							
Tagaya et al. <sup>97</sup>	2010	Breast cancer	Japan	US\$46,000	2010	49,052.93	Cost of device
Unno et al. <sup>98</sup>	2008	Vascular bypass	Japan	€25,000	2008	39,406.12	Cost of device
<b>Other</b>							
Hardesty et al. <sup>102</sup>	2014	Neurosurgery	USA	Cost of dye	2014	Minimal	Per case

<sup>a</sup> Estimated using time-specific currency converter ([www.oanda.com](http://www.oanda.com)) and the Statistical Abstracts of the US ([www.census.gov](http://www.census.gov))

<sup>b</sup> Calculated by subtracting the cost of (blue dye + surgery) from (blue dye + nuclear imaging + surgery)

<sup>c</sup> Based on Medicare Physician Fee Schedule

**FIG. 3** (Left) Schematic of a theranostic nanoparticle. Tumor-specific antibodies are conjugated to ICG-loaded shell containing therapeutic agent. (right) Agent accumulates at tumor providing local therapy and visualization. ICG indocyanine green, CCD charge-coupled device



copyright 2014 jonathan zelken md

## THE FOURTH PARADIGM

The future is bright for molecular NIR fluorescence-guided cancer diagnosis and therapy. Nanoparticles containing NIR-fluorescent dyes were developed that include bioactive ligands which target tumor-specific peptides,

track response to chemotherapy, and deliver therapy (Fig. 3). Sevick-Muraca<sup>118</sup> summarized the state of the art and future directions of nanoparticles, offering examples of tumor-specific detection in head and neck,<sup>13</sup> breast,<sup>119</sup> and prostate cancer.<sup>120</sup> Kolitz-Domb et al. used an ICG-loaded nanoparticle conjugated with anti-carcinoembryonic

antibodies in animal models to accurately detect colon cancers.<sup>6,121</sup> Bahmani et al. studied an ICG-loaded nanoparticle conjugated with anti-HER2 antibodies in a breast cancer model<sup>9</sup>; the molecular construct was more effective at targeting HER2-positive cells than ICG alone or a non-bioactive construct.

Lozano et al. designed a liposomal molecule that encapsulated ICG dye and doxorubicin which accumulated within antibody-specific targets in mice,<sup>7</sup> using multispectral optoacoustic tomography (MSOT) imaging. MSOT interprets sound waves generated by short high-energy bursts of light to generate reliable three-dimensional images.<sup>12</sup> The study illustrated the concept of targeted drug delivery and a method to monitor and track ICG in deep tissue planes. Wang and colleagues used photoacoustic imaging for breast cancer in mice using lipid-encapsulated ICG-loaded nanoparticles with folic acid receptor-targeting ligands, and reported superior tumor-specific imaging compared with unconjugated nanoparticles.<sup>2</sup> Tsujimoto et al. used ICG-loaded tumor-targeted lactosomes to reduce tumor burden in a nude mouse gastric cancer model with photodynamic therapy (PDT).<sup>3</sup> In PDT, an ICG-derived photosensitizer reacts with oxygen and causes target-specific oxidative injury and cell death.<sup>122</sup>

## CONCLUSIONS

The scope of NIR fluorescence-based SLN mapping has since expanded from the breast, skin, lung, stomach, and lower digestive tract to the head and neck, aerodigestive tract, and genitourinary system. The geographic focus of studies has shifted westward from Japan and the Far East, with an expanding role in urology and gynecology. NIR fluorescence imaging plays an important role in SLN mapping, tumor identification, lymphedema diagnosis and management, and reconstructive surgery. There is potential for every stage in surgical oncology. The role of ICG as a diagnostic and therapeutic anti-cancer agent is in preclinical phases and should enhance modern cancer care.

**DISCLOSURES** Jonathan A. Zelken was paid a one-time honorarium to speak on behalf of SwissRay (Taipei, Taiwan) and MediLight (Manila, Philippines), resellers of the Spy Elite Imaging System (Novadaq), on the topic of ICG fluorescence imaging in surgical oncology. He also received an educational grant from Novadaq (manufacturer of the Spy Elite Imaging System) to support fellowship training living expenses.

## REFERENCES

1. Watanabe R, Sato K, Hanaoka H, et al. Minibody-indocyanine green based activatable optical imaging probes: the role of short polyethylene glycol linkers. *ACS Med Chem Lett*. 2014;5(4):411–5.
2. Wang H, Liu C, Gong X, et al. In vivo photoacoustic molecular imaging of breast carcinoma with folate receptor-targeted indocyanine green nanoprobe. *Nanoscale*. 2014;6(23):14270–9.
3. Tsujimoto H, Morimoto Y, Takahata R, et al. Photodynamic therapy using nanoparticle loaded with indocyanine green for experimental peritoneal dissemination of gastric cancer. *Cancer Sci*. 2014;105(12):1626–30.
4. Temma T, Onoe S, Kanazaki K, Ono M, Saji H. Preclinical evaluation of a novel cyanine dye for tumor imaging with in vivo photoacoustic imaging. *J Biomed Opt*. 2014;19(9):090501.
5. Sheng Z, Hu D, Zheng M, et al. Smart human serum albumin-indocyanine green nanoparticles generated by programmed assembly for dual-modal imaging-guided cancer synergistic phototherapy. *ACS Nano*. 2014;8(12):12310–22.
6. Metildi CA, Kaushal S, Luiken GA, Talamini MA, Hoffman RM, Bouvet M. Fluorescently labeled chimeric anti-CEA antibody improves detection and resection of human colon cancer in a patient-derived orthotopic xenograft (PDOX) nude mouse model. *J Surg Oncol*. 2014;109(5):451–8.
7. Lozano N, Al-Ahmady ZS, Beziere NS, Ntziachristos V, Kostarelos K. Monoclonal antibody-targeted PEGylated liposome-ICG encapsulating doxorubicin as a potential theranostic agent. *Int J Pharm*. 2015;482(1–2):2–10.
8. Chi C, Du Y, Ye J, et al. Intraoperative imaging-guided cancer surgery: from current fluorescence molecular imaging methods to future multi-modality imaging technology. *Theranostics*. 2014;4(11):1072–84.
9. Bahmani B, Guerrero Y, Bacon D, Kundra V, Vullev VI, Anvari B. Functionalized polymeric nanoparticles loaded with indocyanine green as theranostic materials for targeted molecular near infrared fluorescence imaging and photothermal destruction of ovarian cancer cells. *Lasers Surg Med*. 2014;46(7):582–92.
10. Ali T, Nakajima T, Sano K, Sato K, Choyke PL, Kobayashi H. Dynamic fluorescent imaging with indocyanine green for monitoring the therapeutic effects of photoimmunotherapy. *Contrast Media Mol Imaging*. 2014;9(4):276–82.
11. Luo S, Zhang E, Su Y, Cheng T, Shi C. A review of NIR dyes in cancer targeting and imaging. *Biomaterials*. 2011;32(29):7127–38.
12. Ntziachristos V, Razansky D. Molecular imaging by means of multispectral optoacoustic tomography (MSOT). *Chem Rev*. 2010;110(5):2783–94.
13. Gleysteen JP, Newman JR, Chhieng D, Frost A, Zinn KR, Rosenthal EL. Fluorescent labeled anti-EGFR antibody for identification of regional and distant metastasis in a preclinical xenograft model. *Head Neck*. 2008;30(6):782–89.
14. Polom K, Murawa D, Rho YS, Nowaczyk P, Hunerbein M, Murawa P. Current trends and emerging future of indocyanine green usage in surgery and oncology: a literature review. *Cancer*. 2011;117(21):4812–22.
15. Xiong L, Gazyakan E, Yang W, et al. Indocyanine green fluorescence-guided sentinel node biopsy: a meta-analysis on detection rate and diagnostic performance. *Eur J Surg Oncol*. 2014;40(7):843–9.
16. Moher D, Liberati A, Tetzlaff J, Altman DG, PRISMA Group. Preferred reporting items for systematic reviews and meta-analyses: the PRISMA statement. *J Clin Epidemiol*. 2009;62(10):1006–12.
17. Polom W, Markuszewski M, Rho YS, Matuszewski M. Use of invisible near infrared light fluorescence with indocyanine green and methylene blue in urology. Part 2. *Cent Eur J Urol*. 2014;67(3):310–3.
18. Polom W, Markuszewski M, Rho YS, Matuszewski M. Usage of invisible near infrared light (NIR) fluorescence with indocyanine green (ICG) and methylene blue (MB) in urological oncology. Part 1. *Cent Eur J Urol*. 2014;67(2):142–8.

19. de Graaf W, Hausler S, Heger M, et al. Transporters involved in the hepatic uptake of (99m)Tc-mebrofenin and indocyanine green. *J Hepatol* 2011;54(4):738–45.
20. Del Vecchio S, Salvatore M. 99mTc-MIBI in the evaluation of breast cancer biology. *Eur J Nucl Med Mol Imaging* 2004;31 Suppl 1:S88–96.
21. Kawaguchi Y, Ishizawa T, Miyata Y, et al. Portal uptake function in veno-occlusive regions evaluated by real-time fluorescent imaging using indocyanine green. *J Hepatol* 2013;58(2):247–53.
22. Ishizawa T, Fukushima N, Shibahara J, et al. Real-time identification of liver cancers by using indocyanine green fluorescent imaging. *Cancer* 2009;115(11):2491–504.
23. Watanabe M, Tsunoda A, Narita K, Kusano M, Miwa M. Colonic tattooing using fluorescence imaging with light-emitting diode-activated indocyanine green: a feasibility study. *Surg Today* 2009;39(3):214–8.
24. Miyashiro I, Hiratsuka M, Sasako M, et al. High false-negative proportion of intraoperative histological examination as a serious problem for clinical application of sentinel node biopsy for early gastric cancer: final results of the Japan Clinical Oncology Group multicenter trial JCOG0302. *Gastric Cancer* 2014;17(2):316–23.
25. Ahmed M, Purushotham AD, Douek M. Novel techniques for sentinel lymph node biopsy in breast cancer: a systematic review. *Lancet Oncol* 2014;15(8):e351–62.
26. Inoue T, Nishi T, Nakano Y, et al. Axillary lymph node recurrence after sentinel lymph node biopsy performed using a combination of indocyanine green fluorescence and the blue dye method in early breast cancer. *Breast Cancer* 2014. doi:10.1007/s12282-014-0573-8.
27. Guo W, Zhang L, Ji J, Gao W, Liu J, Tong M. Evaluation of the benefit of using blue dye in addition to indocyanine green fluorescence for sentinel lymph node biopsy in patients with breast cancer. *World J Surg Oncol* 2014;12:290.
28. Hirano A, Kamimura M, Ogura K, et al. A comparison of indocyanine green fluorescence imaging plus blue dye and blue dye alone for sentinel node navigation surgery in breast cancer patients. *Ann Surg Oncol* 2012;19(13):4112–6.
29. Tong M, Guo W, Gao W. Use of fluorescence imaging in combination with patent blue dye versus patent blue dye alone in sentinel lymph node biopsy in breast cancer. *J Breast Cancer* 2014;17(3):250–5.
30. Verbeek FP, Troyan SL, Mieog JS, et al. Near-infrared fluorescence sentinel lymph node mapping in breast cancer: a multicenter experience. *Breast Cancer Res Treat* 2014;143(2):333–42.
31. Sugie T, Sawada T, Tagaya N, et al. Comparison of the indocyanine green fluorescence and blue dye methods in detection of sentinel lymph nodes in early-stage breast cancer. *Ann Surg Oncol* 2013;20(7):2213–8.
32. Ballardini B, Santoro L, Sangalli C, et al. The indocyanine green method is equivalent to the (99m)Tc-labeled radiotracer method for identifying the sentinel node in breast cancer: a concordance and validation study. *Eur J Surg Oncol* 2013;39(12):1332–6.
33. Samorani D, Fogacci T, Panzini I, et al. The use of indocyanine green to detect sentinel nodes in breast cancer: a prospective study. *Eur J Surg Oncol* 2015;41(1):64–70.
34. Thompson M, Korourian S, Henry-Tillman R, et al. Axillary reverse mapping (ARM): a new concept to identify and enhance lymphatic preservation. *Ann Surg Oncol* 2007;14(6):1890–5.
35. Nos C, Lesieur B, Clough KB, Lecuru F. Blue dye injection in the arm in order to conserve the lymphatic drainage of the arm in breast cancer patients requiring an axillary dissection. *Ann Surg Oncol* 2007;14(9):2490–6.
36. Sakurai T, Endo M, Shimizu K, et al. Axillary reverse mapping using fluorescence imaging is useful for identifying the risk group of postoperative lymphedema in breast cancer patients undergoing sentinel node biopsies. *J Surg Oncol* 2014;109(6):612–5.
37. Ikeda K, Ogawa Y, Kajino C, et al. The influence of axillary reverse mapping related factors on lymphedema in breast cancer patients. *Eur J Surg Oncol* 2014;40(7):818–23.
38. Noguchi M, Noguchi M, Nakano Y, Ohno Y, Kosaka T. Axillary reverse mapping using a fluorescence imaging system in breast cancer. *J Surg Oncol* 2012;105(3):229–34.
39. Noguchi M, Yokoi M, Nakano Y. Axillary reverse mapping with indocyanine fluorescence imaging in patients with breast cancer. *J Surg Oncol* 2010;101(3):217–21.
40. Noguchi M, Miura S, Morioka E, et al. Is axillary reverse mapping feasible in breast cancer patients? *Eur J Surg Oncol* 2015;41(4):442–9.
41. Cheng MH, Chen SC, Henry SL, Tan BK, Lin MC, Huang JJ. Vascularized groin lymph node flap transfer for postmastectomy upper limb lymphedema: flap anatomy, recipient sites, and outcomes. *Plast Reconstr Surg* 2013;131(6):1286–98.
42. Ito R, Suami H. Overview of lymph node transfer for lymphedema treatment. *Plast Reconstr Surg* 2014;134(3):548–56.
43. Patel KM, Lin CY, Cheng MH. From theory to evidence: long-term evaluation of the mechanism of action and flap integration of distal vascularized lymph node transfers. *J Reconstr Microsurg* 2015;31(1):26–30.
44. Raju A, Chang DW. Vascularized lymph node transfer for treatment of lymphedema: a comprehensive literature review. *Ann Surg* 2015;261(5):1013–23.
45. Torrisi JS, Joseph WJ, Ghanta S, et al. Lymphaticovenous bypass decreases pathologic skin changes in upper extremity breast cancer-related lymphedema. *Lymphat Res Biol* 2015;13(1):46–53.
46. Patel KM, Lin CY, Cheng MH. A prospective evaluation of lymphedema-specific quality-of-life outcomes following vascularized lymph node transfer. *Ann Surg Oncol* 2015;22(7):2424–30.
47. Vignes S, Blanchard M, Yannoutsos A, Arrault M. Complications of autologous lymph-node transplantation for limb lymphoedema. *Eur J Vasc Endovasc Surg* 2013;45(5):516–20.
48. Viitanen TP, Maki MT, Seppanen MP, Suominen EA, Saaristo AM. Donor-site lymphatic function after microvascular lymph node transfer. *Plast Reconstr Surg* 2012;130(6):1246–53.
49. Dayan JH, Dayan E, Smith ML. Reverse lymphatic mapping: a new technique for maximizing safety in vascularized lymph node transfer. *Plast Reconstr Surg* 2015;135(1):277–85.
50. Tummers QR, Verbeek FP, Schaafsma BE, et al. Real-time intraoperative detection of breast cancer using near-infrared fluorescence imaging and Methylene Blue. *Eur J Surg Oncol* 2014;40(7):850–8.
51. Murphy MP. Targeting lipophilic cations to mitochondria. *Biochim Biophys Acta* 2008;1777(7–8):1028–31.
52. Madajewski B, Judy BF, Mouchli A, et al. Intraoperative near-infrared imaging of surgical wounds after tumor resections can detect residual disease. *Clin Cancer Res* 2012;18(20):5741–51.
53. Harada N, Ishizawa T, Muraoka A, et al. Fluorescence navigation hepatectomy by visualization of localized cholestasis from bile duct tumor infiltration. *J Am Coll Surg* 2010;210(6):e2–6.
54. Ishizawa T, Masuda K, Urano Y, et al. Mechanistic background and clinical applications of indocyanine green fluorescence imaging of hepatocellular carcinoma. *Ann Surg Oncol* 2014;21(2):440–8.
55. van der Vorst JR, Schaafsma BE, Hutteman M, et al. Near-infrared fluorescence-guided resection of colorectal liver metastases. *Cancer* 2013;119(18):3411–8.
56. Lim C, Vibert E, Azoulay D, et al. Indocyanine green fluorescence imaging in the surgical management of liver cancers:

- current facts and future implications. *J Visc Surg.* 2014;151(2):117–24.
57. Tummers QR, Verbeek FP, Prevoo HA, et al. First experience on laparoscopic near-infrared fluorescence imaging of hepatic uveal melanoma metastases using indocyanine green. *Surg Innov.* 2015;22(1):20–5.
  58. Gilmore DM, Khullar OV, Gioux S, et al. Effective low-dose escalation of indocyanine green for near-infrared fluorescent sentinel lymph node mapping in melanoma. *Ann Surg Oncol.* 2013;20(7):2357–63.
  59. Korn JM, Tellez-Diaz A, Bartz-Kurycki M, Gastman B. Indocyanine green SPY elite-assisted sentinel lymph node biopsy in cutaneous melanoma. *Plast Reconstr Surg.* 2014;133(4):914–22.
  60. van der Vorst JR, Schaafsma BE, Verbeek FP, et al. Dose optimization for near-infrared fluorescence sentinel lymph node mapping in patients with melanoma. *Br J Dermatol.* 2013;168(1):93–98.
  61. Jain V, Phillips BT, Conkling N, Pameijer C. Sentinel lymph node detection using laser-assisted indocyanine green dye lymphangiography in patients with melanoma. *Int J Surg Oncol.* 2013;2013:904214.
  62. Fujiwara M, Mizukami T, Suzuki A, Fukamizu H. Sentinel lymph node detection in skin cancer patients using real-time fluorescence navigation with indocyanine green: preliminary experience. *J Plast Reconstr Aesthet Surg.* 2009;62(10):e373–8.
  63. Stoffels I, von der Stuck H, Boy C, et al. Indocyanine green fluorescence-guided sentinel lymph node biopsy in dermatology. *J Dtsch Dermatol Ges.* 2012;10(1):51–7.
  64. Namikawa K, Yamazaki N. Sentinel lymph node biopsy guided by indocyanine green fluorescence for cutaneous melanoma. *Eur J Dermatol.* 2011;21(2):184–90.
  65. Fujisawa Y, Nakamura Y, Kawachi Y, Otsuka F. Indocyanine green fluorescence-navigated sentinel node biopsy showed higher sensitivity than the radioisotope or blue dye method, which may help to reduce false-negative cases in skin cancer. *J Surg Oncol.* 2012;106(1):41–5.
  66. Cloyd JM, Wapnir IL, Read BM, Swetter S, Greco RS. Indocyanine green and fluorescence lymphangiography for sentinel lymph node identification in cutaneous melanoma. *J Surg Oncol.* 2014;110(7):888–92.
  67. van der Vorst JR, Schaafsma BE, Verbeek FP, et al. Randomized comparison of near-infrared fluorescence imaging using indocyanine green and 99(m) technetium with or without patent blue for the sentinel lymph node procedure in breast cancer patients. *Ann Surg Oncol.* 2012;19(13):4104–11.
  68. van der Pas MH, Ankersmit M, Stockmann HB, et al. Laparoscopic sentinel lymph node identification in patients with colon carcinoma using a near-infrared dye: description of a new technique and feasibility study. *J Laparoendosc Adv Surg Tech A.* 2013;23(4):367–71.
  69. Miyashiro I, Hiratsuka M, Kishi K, et al. Intraoperative diagnosis using sentinel node biopsy with indocyanine green dye in gastric cancer surgery: an institutional trial by experienced surgeons. *Ann Surg Oncol.* 2013;20(2):542–6.
  70. Noura S, Ohue M, Seki Y, et al. Feasibility of a lateral region sentinel node biopsy of lower rectal cancer guided by indocyanine green using a near-infrared camera system. *Ann Surg Oncol.* 2010;17(1):144–51.
  71. Hirche C, Dresel S, Krempien R, Hunerbein M. Sentinel node biopsy by indocyanine green retention fluorescence detection for inguinal lymph node staging of anal cancer: preliminary experience. *Ann Surg Oncol.* 2010;17(9):2357–62.
  72. Kumagai Y, Ishiguro T, Haga N, Kuwabara K, Kawano T, Ishida H. Hemodynamics of the reconstructed gastric tube during esophagectomy: assessment of outcomes with indocyanine green fluorescence. *World J Surg.* 2014;38(1):138–43.
  73. Pacheco PE, Hill SM, Henriques SM, Paulsen JK, Anderson RC. The novel use of intraoperative laser-induced fluorescence of indocyanine green tissue angiography for evaluation of the gastric conduit in esophageal reconstructive surgery. *Am J Surg.* 2013;205(3):349–52. (discussion 352–343).
  74. Rino Y, Yukawa N, Sato T, et al. Visualization of blood supply route to the reconstructed stomach by indocyanine green fluorescence imaging during esophagectomy. *BMC Med Imaging.* 2014;14:18.
  75. Shimada Y, Okumura T, Nagata T, et al. Usefulness of blood supply visualization by indocyanine green fluorescence for reconstruction during esophagectomy. *Esophagus.* 2011;8(4):259–66.
  76. Handgraaf HJ, Verbeek FP, Tummers QR, et al. Real-time near-infrared fluorescence guided surgery in gynecologic oncology: a review of the current state of the art. *Gynecol Oncol.* 2014;135(3):606–13.
  77. Jewell EL, Huang JJ, Abu-Rustum NR, et al. Detection of sentinel lymph nodes in minimally invasive surgery using indocyanine green and near-infrared fluorescence imaging for uterine and cervical malignancies. *Gynecol Oncol.* 2014;133(2):274–7.
  78. Crane LM, Themelis G, Arts HJ, et al. Intraoperative near-infrared fluorescence imaging for sentinel lymph node detection in vulvar cancer: first clinical results. *Gynecol Oncol.* 2011;120(2):291–5.
  79. Sinno AK, Fader AN, Roche KL, Giuntoli RL 2nd, Tanner EJ. A comparison of colorimetric versus fluorometric sentinel lymph node mapping during robotic surgery for endometrial cancer. *Gynecol Oncol.* 2014;134(2):281–6.
  80. Ohnishi S, Lomnes SJ, Laurence RG, Gogbashian A, Mariani G, Frangioni JV. Organic alternatives to quantum dots for intraoperative near-infrared fluorescent sentinel lymph node mapping. *Mol Imaging.* 2005;4(3):172–81.
  81. Schaafsma BE, Verbeek FP, Peters AA, et al. Near-infrared fluorescence sentinel lymph node biopsy in vulvar cancer: a randomised comparison of lymphatic tracers. *BJOG.* 2013;120(6):758–64.
  82. Schaafsma BE, Verbeek FP, Elzevier HW, et al. Optimization of sentinel lymph node mapping in bladder cancer using near-infrared fluorescence imaging. *J Surg Oncol.* 2014;110(7):845–50.
  83. Manny TB, Patel M, Hemal AK. Fluorescence-enhanced robotic radical prostatectomy using real-time lymphangiography and tissue marking with percutaneous injection of unconjugated indocyanine green: the initial clinical experience in 50 patients. *Eur Urol.* 2014;65(6):1162–8.
  84. Yamashita S, Tokuishi K, Anami K, et al. Video-assisted thoracoscopic indocyanine green fluorescence imaging system shows sentinel lymph nodes in non-small-cell lung cancer. *J Thorac Cardiovasc Surg.* 2011;141(1):141–4.
  85. Sugi K, Fukuda M, Nakamura H, Kaneda Y. Comparison of three tracers for detecting sentinel lymph nodes in patients with clinical N0 lung cancer. *Lung Cancer.* 2003;39(1):37–40.
  86. Bille A, Pelosi E, Skanjeti A, et al. Preoperative intrathoracic lymph node staging in patients with non-small-cell lung cancer: accuracy of integrated positron emission tomography and computed tomography. *Eur J Cardiothorac Surg.* 2009;36(3):440–5.
  87. Yamashita S, Tokuishi K, Miyawaki M, et al. Sentinel node navigation surgery by thoracoscopic fluorescence imaging system and molecular examination in non-small cell lung cancer. *Ann Surg Oncol.* 2012;19(3):728–33.
  88. Gilmore DM, Khullar OV, Jaklitsch MT, Chirieac LR, Frangioni JV, Colson YL. Identification of metastatic nodal disease in a phase 1 dose-escalation trial of intraoperative sentinel lymph node mapping in non-small cell lung cancer using near-infrared

- imaging. *J Thorac Cardiovasc Surg.* 2013;146(3):562–70. (discussion 569–570).
89. Okusanya OT, Holt D, Heitjan D, et al. Intraoperative near-infrared imaging can identify pulmonary nodules. *Ann Thorac Surg.* 2014;98(4):1223–30.
  90. Yokoyama J, Fujimaki M, Ohba S, et al. A feasibility study of NIR fluorescent image-guided surgery in head and neck cancer based on the assessment of optimum surgical time as revealed through dynamic imaging. *Onco Targets Ther.* 2013;6:325–330.
  91. Ohba S, Yokoyama J, Fujimaki M, et al. Significant improvement in superselective intra-arterial chemotherapy for oral cancer by using indocyanine green fluorescence. *Oral Oncol.* 2012;48(11):1101–5.
  92. Yokoyama J, Ohba S, Fujimaki M, Kojima M, Suzuki M, Ikeda K. Significant improvement in superselective intra-arterial chemotherapy for advanced paranasal sinus cancer by using indocyanine green fluorescence. *Eur Arch Otorhinolaryngol.* 2014;271(10):2795–801.
  93. Hao S, Li D, Ma G, Yang J, Wang G. Application of intraoperative indocyanine green videoangiography for resection of spinal cord hemangioblastoma: advantages and limitations. *J Clin Neurosci.* 2013;20(9):1269–75.
  94. Holt D, Okusanya O, Judy R, et al. Intraoperative near-infrared imaging can distinguish cancer from normal tissue but not inflammation. *PLoS One.* 2014;9(7):e103342.
  95. Chang SB, Askew RL, King Y, et al. Prospective assessment of postoperative complications and associated costs following inguinal lymph node dissection (ILND) in melanoma patients. *Ann Surg Oncol.* 2010;17(10):2764–72.
  96. Morton DL, Cochran AJ, Thompson JF, et al. Sentinel node biopsy for early-stage melanoma: accuracy and morbidity in MSLT-I, an international multicenter trial. *Ann Surg.* 2005;242(3):302–11. (discussion 311–303).
  97. Tagaya N, Tsumuraya M, Nakagawa A, Iwasaki H, Kato H, Kubota K. Indocyanine green (ICG) fluorescence imaging versus radioactive colloid for sentinel lymph node identification in patients with breast cancer [abstract no. 674]. *J Clin Oncol.* 2010;28(15 Suppl):674.
  98. Unno N, Suzuki M, Yamamoto N, et al. Indocyanine green fluorescence angiography for intraoperative assessment of blood flow: a feasibility study. *Eur J Vasc Endovasc Surg.* 2008;35(2):205–7.
  99. Chatterjee A, Krishnan NM, Van Vliet MM, Powell SG, Rosen JM, Ridgway EB. A comparison of free autologous breast reconstruction with and without the use of laser-assisted indocyanine green angiography: a cost-effectiveness analysis. *Plast Reconstr Surg.* 2013;131(5):693e–701e.
  100. Duggal CS, Madni T, Losken A. An outcome analysis of intraoperative angiography for postmastectomy breast reconstruction. *Aesthet Surg J.* 2014;34(1):61–65.
  101. Kanuri A, Liu AS, Guo L. Whom should we SPY? A cost analysis of laser-assisted indocyanine green angiography in prevention of mastectomy skin flap necrosis during prosthesis-based breast reconstruction. *Plast Reconstr Surg.* 2014;133(4):448e–54e.
  102. Hardesty DA, Thind H, Zabramski JM, Spetzler RF, Nakaji P. Safety, efficacy, and cost of intraoperative indocyanine green angiography compared to intraoperative catheter angiography in cerebral aneurysm surgery. *J Clin Neurosci.* 2014;21(8):1377–82.
  103. Govers TM, Takes RP, Baris Karakullukcu M, et al. Management of the N0 neck in early stage oral squamous cell cancer: a modeling study of the cost-effectiveness. *Oral Oncol.* 2013;49(8):771–7.
  104. Jakovljevic M, Zucic A, Rankovic A, Dagovic A. Radiation therapy remains the key cost driver of oncology inpatient treatment. *J Med Econ.* 2015;18(1):29–36.
  105. Martinez-Menchon T, Sanchez-Pedreno P, Martinez-Escribano J, Corbalan-Velez R, Martinez-Barba E. Cost analysis of sentinel lymph node biopsy in melanoma. *Actas Dermosifiliogr.* 2015;106(3):201–7.
  106. McCann GA, Cohn DE, Jewell EL, Havrilesky LJ. Lymphatic mapping and sentinel lymph node dissection compared to complete lymphadenectomy in the management of early-stage vulvar cancer: a cost-utility analysis. *Gynecol Oncol.* 2015;136(2):300–4.
  107. McMasters KM, Wong SL, Tuttle TM, et al. Preoperative lymphoscintigraphy for breast cancer does not improve the ability to identify axillary sentinel lymph nodes. *Ann Surg.* 2000;231(5):724–31.
  108. Meads C, Sutton A, Malysiak S, et al. Sentinel lymph node status in vulvar cancer: systematic reviews of test accuracy and decision-analytic model-based economic evaluation. *Health Technol Assess.* 2013;17(60):1–216.
  109. O'Connor R, Pezier T, Schilling C, McGurk M. The relative cost of sentinel lymph node biopsy in early oral cancer. *J Craniomaxillofac Surg.* 2013;41(8):721–7.
  110. Thompson M, Korourian S, Henry-Tillman R, et al. Intraoperative radioisotope injection for sentinel lymph node biopsy. *Ann Surg Oncol.* 2008;15(11):3216–21.
  111. Yeoh MS, Kim DD, Ghali GE. Fluorescence angiography in the assessment of flap perfusion and vitality. *Oral Maxillofac Surg Clin North Am.* 2013;25(1):61–66, vi.
  112. Komorowska-Timek E, Gurtner GC. Intraoperative perfusion mapping with laser-assisted indocyanine green imaging can predict and prevent complications in immediate breast reconstruction. *Plast Reconstr Surg.* 2010;125(4):1065–73.
  113. Newman MI, Samson MC, Tamburrino JF, Swartz KA. Intraoperative laser-assisted indocyanine green angiography for the evaluation of mastectomy flaps in immediate breast reconstruction. *J Reconstr Microsurg.* 2010;26(7):487–92.
  114. Moyer HR, Losken A. Predicting mastectomy skin flap necrosis with indocyanine green angiography: the gray area defined. *Plast Reconstr Surg.* 2012;129(5):1043–8.
  115. Newman MI, Jack MC, Samson MC. SPY-Q analysis toolkit values potentially predict mastectomy flap necrosis. *Ann Plast Surg.* 2013;70(5):595–8.
  116. Holm C, Dornseifer U, Sturtz G, Ninkovic M. Sensitivity and specificity of ICG angiography in free flap reexploration. *J Reconstr Microsurg.* 2010;26(5):311–6.
  117. Khansa I, Chao AH, Taghizadeh M, Nagel T, Wang D, Tiwari P. A systematic approach to emergent breast free flap takeback: Clinical outcomes, algorithm, and review of the literature. *Microsurgery.* 2013;33(7):505–13.
  118. Sevic-Muraca EM. Translation of near-infrared fluorescence imaging technologies: emerging clinical applications. *Annu Rev Med.* 2012;63:217–31.
  119. Sampath L, Kwon S, Hall MA, Price RE, Sevic-Muraca EM. Detection of cancer metastases with a dual-labeled near-infrared/positron emission tomography imaging agent. *Transl Oncol.* 2010;3(5):307–17.
  120. Hall MA, Kwon S, Robinson H, et al. Imaging prostate cancer lymph node metastases with a multimodality contrast agent. *Prostate.* 2012;72(2):129–46.
  121. Kollitz-Domb M, Grinberg I, Corem-Salkmon E, Margel S. Engineering of near infrared fluorescent proteinoid-poly(L-lactic acid) particles for in vivo colon cancer detection. *J Nanobiotechnology.* 2014;12:30.
  122. Belichenko I, Morishima N, Separovic D. Caspase-resistant vimentin suppresses apoptosis after photodynamic treatment with a silicon phthalocyanine in Jurkat cells. *Arch Biochem Biophys.* 2001;390(1):57–63.